ISSN: 2278-0181
Vol. 2 Issue 11, November - 2013

Directional Stiffness of Electronic Component Lead

Chang H. Kim

California State University, Long Beach
Department of Mechanical and Aerospace Engineering
1250 Bellflower Boulevard
Long Beach, CA 90840-830, USA

Abstract

It has been known that the lead stiffness or compliance of surface mounted electronic components is one of the key parameters in predicting the long-term solder joint reliability under a thermal cyclic environment. Thus, computing an accurate lead stiffness value is essential, especially for the corner lead stiffness along the diagonal direction of the component because the corner leads will experience the most deformation. The angle measured from the lead body coordinate system to the diagonal direction of the components will be varied depending on the component geometry, and thus, formulation of stiffness variation with respect to the angle change is also highly desirable. Such off-axis stiffness is generally known as the directional stiffness. An accurate closed-form solution to compute the directional lead stiffness of the surface mounted electronic components will be presented here. The solution will be based on two in-plane stiffness values along the lead body coordinate system parallel to the substrate. The comparison between the theoretical and computational solutions is shown to be in excellent agreement.

1. Introduction

One of the key parameters in lead design for surface mounted components (SMC) is the stiffness or compliance of the lead under the thermal cycling environment. Due to the thermal mismatch between the SMC and its substrate, such as a printed circuit board (PCB), the interacting stress may rise and transmit to the weaker solder joint that in turn may fail due to fatigue. It is generally known that stiffer leads tend to reduce the number of thermal cycles required to fail a solder joint, and thus, shortens the thermal life expectancy of the SMC [1-9].

The efforts to compute lead stiffness continued. Gee and van Kessel approximated the stiffness of the curved lead by using simple beam bending theory [7] while Kotlowitz et al computed the lead stiffness of various sizes and shapes by using classical elastic strain energy methods [2-6].

Six stiffness values per lead end can be obtained along its body coordinate system where Lau and Harkins used FEA technique to provide a full 12x12 stiffness matrix of a lead which could relate stress resultants to the deformation field at both ends of the lead [9].

When the SMC and the PCB expand at their own rates during thermal cycling, the corner leads undergo the largest dimensional changes since they are at the farthest distance away from the geometric center of the SMC. Since the corner leads will experience the most deformation, they are considered to be the critical leads. They will deform along the direction from the geometric center of the SMC to the location of the corner lead position. This direction is at an angle to the lead body coordinate system. Such off-axis stiffness will be called the directional stiffness. It is important to compute the accurate directional stiffness of the corner leads where the off-axis angle depends on the geometry of the components. Substrate warping during low-frequency temperature cycling is assumed to be negligible.

Kotlowitz formulated the directional stiffness in [2]. However, the directional stiffness along the diagonal of a SMC was shown to have 6% deviation from the FEA result. The effort to upgrade the diagonal stiffness accuracy can be seen in [3], but similar differences still existed.

The primary objective is to provide an accurate formulation to compute the directional stiffness of the corner leads. In fact, the general formulation and its concept can be applicable to many other structural elements. The validity of the formulation is tested with a given SMC lead geometry by the finite element method. It will be shown that the theoretical prediction matches very well with the corresponding finite element solutions.

2. Directional Lead Stiffness

2.1. General Concept

The body coordinate system for a structural element such as a lead of a SMC is shown in Fig. 1 where the x and y axis are parallel to the substrate, and the z-axis is defined perpendicular to the substrate. Out of 6 stiffness values, two stiffness values, k_x and k_y, are used to compute the directional stiffness, k_r. The stiffness, k_x and k_y, represent in-plane stiffness of the lead along the x and y directions, respectively, and the directional stiffness, k_r, represents the stiffness along the r-direction. The main objective is to formulate the directional stiffness (k_r) based on known in-plane stiffness, k_x and k_y, and the given r-direction.

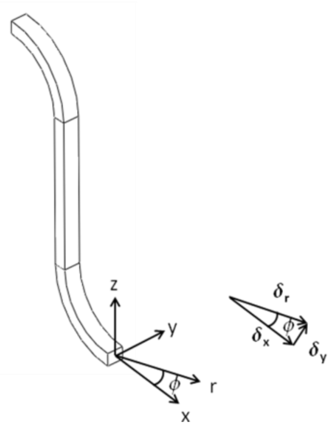

Fig. 1. Lead body coordinate system at the lead end. The x and y-axes are in-plane to the substrate, and the z-axis is perpendicular to the substrate.

From Fig. 1, the r-direction is defined to be at an angle (ϕ) from the x-axis. While the upper end of the lead is held fixed, the other lead end is displaced by δ_r along the r-direction. Then,

$$\delta_r^2 = \delta_x^2 + \delta_y^2 \tag{1}$$

where δ_x and δ_y are deformations along the x and y directions, respectively. The following relations can also be established from Fig. 1,

$$\sin\phi = \frac{\delta_y}{\delta_r} \tag{2}$$

$$\cos\phi = \frac{\delta_x}{\delta_r} \tag{3}$$

And, let tan(ϕ)=R,

$$\tan\phi = \frac{\delta_y}{\delta_x} = R \tag{4}$$

After substituting δ_r from (1) into (2), and rewriting the equation in term of R,

$$\sin\phi = \frac{R}{\sqrt{1+R^2}} \tag{5}$$

Similarly for (3),

$$\cos\phi = \frac{1}{\sqrt{1+R^2}} \tag{6}$$

It is also noted that the resultant force (F_r) induced by δ_r in the r-direction is related to its component forces (F_x and F_y) in the x and y directions. Thus,

$$F_r^2 = F_x^2 + F_y^2 \tag{7}$$

where by definition

$$F_r = k_r \cdot \delta_r \tag{8a}$$

$$F_x = k_x \cdot \delta_x \tag{8b}$$

$$F_y = k_y \cdot \delta_y \tag{8c}$$

After substituting (8) into (7), and then dividing by δ_r using the relation shown in (1), (5), and (6), k_r can now be derived as follows,

$$k_r = \sqrt{\frac{k_x^2 + R^2 k_y^2}{1+R^2}} \tag{9}$$

The equation shown in (9) states that for a given structural element, when in-plane stiffness, k_x and k_y, and R are known, the directional stiffness can be found. It can also be deduced from (9), the directional stiffness k_r is same for +ϕ and –ϕ with respect to the x-axis due to R^2 term.

As $R \rightarrow 0$ (or the angle ϕ approaches 0°), k_r becomes k_x, and as $R \rightarrow \infty$ (or the angle ϕ approaches 90°), k_r becomes k_y. For $R \rightarrow 1$ (or the angle ϕ approaches 45°), $k_r = \sqrt{k_x^2 + k_y^2} / \sqrt{2}$.

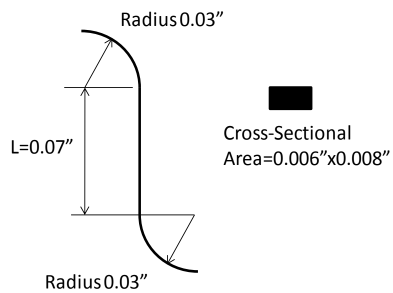

Fig. 2. Structural model for S-shaped (gull-wing type) lead geometry

A simplified S-shaped lead geometry of the gull-wing types is shown in Fig. 2 which will be used for the upcoming illustrations. The lead overall height is approximately 0.13" and its cross-sectional area is shown to be 0.006"x0.008". The simple finite element beam model was created where the fixed boundary condition is applied at one end of the lead, and the unit displacement is prescribed at the other end. The lead material, Kovar, with elastic modulus of 2.2×10^7 psi and Poisson's ratio of 0.35, is chosen.

From the FEA, the stiffness value for the given lead geometry can be computed simply by dividing the reaction load by the prescribed displacement in the desired direction. First, the in-plane stiffness values, k_x and k_y, of the lead must be found. They can be obtained by either FEA or the classical elastic strain energy methods given in [2,3]. For simplicity, the in-plane stiffness values for k_x=3.15 lb/in and k_y=3.59 lb/in are computed. However, these values are verified to be within 0.5% difference between the FEA and the classical methods from [2,3]. Since the difference is acceptable for this engineering application, k_x=3.15 lb/in and k_y=3.59 lb/in will be used to compute k_r. Fig. 3 plots the directional stiffness obtained by (9) with respect to the inclined angle ϕ.

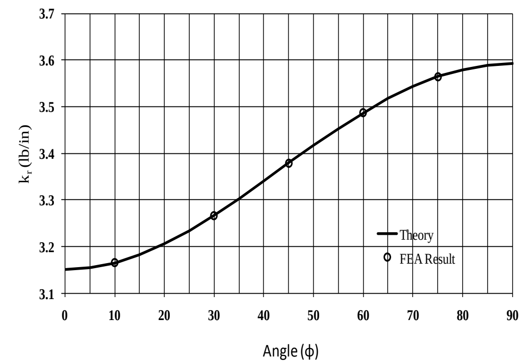

Fig. 3. Comparison between theoretical and FEA solution. (k_x=3.15 lb/in and k_y=3.59 lb/in)

Five additional FEA stiffness values are computed at ϕ=10°, 30°, 45°, 60°, and 75°. For comparison, the FEA results are also plotted in Fig. 3 which shows excellent agreement with the theoretical prediction. The difference between the theory and computation solution is shown to be less than 0.016% at ϕ=45°. Similarly, when the computational result at ϕ=45° is compared to the directional stiffness calculated by the method given in [3], it only shows a difference of 0.8% at ϕ=45°. However, this is because both in-plane stiffness values are comparable, k_x=3.15 lb/in and k_y=3.59 lb/in.

For a lead that has dissimilar in-plane stiffness values, the difference between the method from [3] and computational solutions will become significant. Another example can be illustrated by simply changing the cross sectional area from 0.006"x0.008" to 0.006"x0.012". Then, k_x=4.72 lb/in and k_y=8.93 lb/in are obtained for the larger cross sectional area. In this case, the directional stiffness at ϕ=45° calculated by the method shown in [3] is under-predicted by 13.5% when compared to the FEA result. A few data points are tabulated in Table 1 for further comparison. The difference between the FEA results and theoretical prediction by (9) is shown to be negligible.

TABLE I
Directional Stiffness Comparison
(k_x=4.72 lb/in and k_y=8.93 lb/in)

Angle (ϕ)	Directional Stiffness (lb/in)			
	Eq. (9)	FEA	Ref. [2]	Ref. [3]
10	4.91	4.91	4.78	4.79
30	6.06	6.06	5.22	5.36
45	7.15	7.14	5.91	6.18
60	8.09	8.09	6.97	7.31
75	8.71	8.71	8.25	8.43

2.2. Application to Surface Mounted Component

A surface mounted component (SMC) comes in many different sizes and shapes. Such a typical SMC can be seen in Fig. 4 where the *u*-axis and *v*-axis represent the SMC coordinate system or simply the *u*-*v* coordinate system. Since the corner leads undergo the largest deformation, two representative corner leads are shown in Fig. 4 and 5. The corner lead position 1 in Fig.4 shows that the lead body coordinate system is parallel to the component coordinate system. The angle ϕ_1 is inclined from the x-axis and as well as from *u*-axis, and $\tan(\phi_1)$ can be found by its coordinate (u_1,v_1) measured from the origin of the *u*-*v* coordinate system.

$$\tan\phi_1 = \frac{v_1}{u_1} = R_1 \qquad (10)$$

And thus, the corresponding directional stiffness at the corner lead position 1 can be written directly from (9),

$$k_{r,position1} = \sqrt{\frac{k_x^2 + R_1^2 k_y^2}{1+R_1^2}} \qquad (11)$$

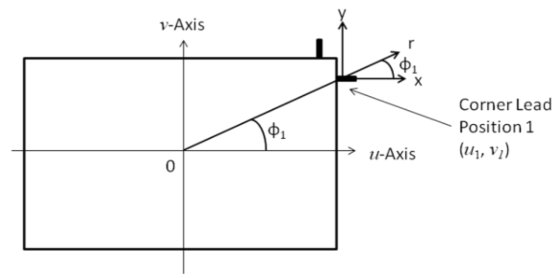

Fig. 4. The geometry of the corner lead at position 1. The coordinate (u_1, v_1) are measured from the origin of the *u*-*v* coordinate system.

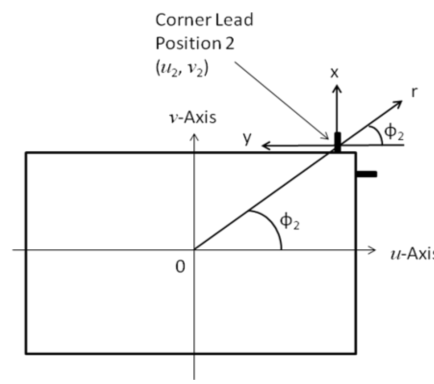

Fig. 5. The geometry of the corner lead at position 2. The coordinate (u_2, v_2) are measured from the origin of the *u*-*v* coordinate system.

Fig. 5 shows the location of the corner lead position 2 with its related geometry. The lead body coordinate system at position 2 is rotated by 90 degrees from the *u*-axis, and the angle ϕ_2 is shown to be inclined from the y-axis of the lead body coordinate system. Similarly,

$$\tan\phi_2 = \frac{v_2}{u_2} = R_2 \qquad (12)$$

where (u_2, v_2) is the coordinate measured from the origin of the *u*-*v* coordinate system for the corner lead position 2. After re-deriving the directional stiffness as shown before, the directional stiffness at the corner lead position 2 can now be written as follows,

$$k_{r,position2} = \sqrt{\frac{R_2^2 k_x^2 + k_y^2}{1+R_2^2}} \quad (13)$$

The formulation in (13) can also be derived from (10) and (11) by simply replacing $\phi_1 = 90 - \phi_2$ and $R_1 = 1/R_2$.

The definition of R_1 and R_2 as shown in (10) and (12) are essentially the same, and thus, R can replace R_1 and R_2 for simplicity.

3. Closing Remark

The mathematical formulation in predicting the directional stiffness of the structural element, such as electronic component leads, has been significantly improved. An excellent agreement was shown when comparing theoretical and computational solutions for the diagonal stiffness values of a surface mounted component lead.

4. References

[1] W. Englemaier and A. I. Attarwala "Surface-mount attachment reliability of clip-leaded ceramic chip carriers on FR-4 circuit board", *IEEE Tran. Components, Hybrids, and Manufacturing Technology*, vol. 12, no. 2, June. 1989, pp. 284-296.

[2] R. W. Kotlowitz, "Comparative compliance of representative lead designs for surface mounted components", *IEEE Tran. Components, Hybrids, and Manufacturing Technology*, vol. 12, no. 4, Dec. 1989, pp. 431-448.

[3] R. W. Kotlowitz, "Compliance metrics for surface mount component lead design", Proceedings 1990 IEEE Electronic Components and Technology Conference, Las Vegas, NV, May 21-23, 1990, vol. 2, pp. 1054-1063.

[4] R. W. Kotlowitz and L. R. Taylor, "Compliance metrics for the inclined gull-wing, spider J-bend, and spider gull-wing lead designs for surface mount components", *IEEE Tran. Components, Hybrids, and Manufacturing Technology*, vol. 14, no. 4, Dec. 1991, pp. 771-779.

[5] R. W. Kotlowitz and G. Gosen, "Compliance metrics for the generalized S-bend lead design for surface mount components", Proceedings 1992 IEEE Electronic Components and Technology Conference, San Diego, CA, May 18-20, 1992, pp. 345-353.

[6] R. W. Kotlowitz and I. M. Nevarez, "Compliance metrics for the S-bend lead design for surface mount components with application to clip-leads", Proceedings 1993 IEEE Electronic Components and Technology Conference, Orlando, Fl, June 1-4, 1993, pp. 1104-1114.

[7] S. A. Gee and C.G.M. van Kessel, "Stiffness and yielding in PLCC "J" lead", *IEEE Tran. Components, Hybrids, and Manufacturing Technology*, vol. CHMT-10, no. 3, Sept. 1987, pp. 379-390.

[8] W. E. Jahsman and P. Jain, "Comparison of predicted and measured lead stiffnesses of surface mounted packages", Proceedings 40th Components and Technology conference, 1990, pp. 926-932.

[9] J. H. Lau and C. G. Harkins, "Stiffness of "gull-wing" leads and solder joints for a plastic quad flat pack", *IEEE Tran. Components, Hybrids, and Manufacturing Technology*, vol. 13, no. 1, Mar. 1990, pp. 124-130.